Turbulence Structure of Dilute Drag-Reducing Polymer Solutions in a Rectangular Open Channel Flow

The drag reduction phenomenon in a rectangular open channel flow was examined by measuring the longitudinal velocity by means of a laser Doppler anemometer. Statistical analysis of the fluctuating velocity showed that the most significant effect of the polymer additive (polyethylene oxide) on the large-scale turbulent motion appeared in the turbulent core of an open channel flow. The scale of bursting phenomenon was enlarged by the polymer additive, and the typical ejection process was detected as the remarkable negative fluctuating velocity throughout the buffer and turbulent core regions except near the free surface.

HIROMOTO USUI and YUJI SANO

Department of Chemical Engineering
Yamaguchi University
Ube 755, Japan

SCOPE

While drag reduction phenomenon in pipe flows is well documented, little has been reported on the application of this phenomenon to an open channel flow. Sellin and Barnard (1970), Sellin and Ollis (1979), and Usui and Irvine (1980) showed that drag reduction with polymer additives was effective in the storm sewer system when there existed danger of system overloading. However, the mechanism of drag reduction in an open channel flow is not well known at the present stage.

The principal object of this work was to provide the experimental results for turbulent flow characteristics of drag-reducing polymer solutions in an open channel. An open channel flow has the characteristics both of wall bounded flow and of free surface flow. The effect of free surface on the turbulence structure in an open channel flow was most interesting because the previous work in turbulent pipe flows did not contain this effect. A laser Doppler anemometer was employed to measure the longitudinal fluctuating velocity. To simplify the problem in a water sewer, a rectangular open channel with large aspect ratio was used to provide essentially a two dimensional flow.

CONCLUSION AND SIGNIFICANCE

Drag reduction in a rectangular open channel flow was detected using 50 and 100 ppm polymer additives (polyethylene oxide, molecular weight was around 4×10^6). Although the scale-up problem was not discussed in this work, the maximum increase of discharge capacity was 40% of the Newtonian fluid case.

The turbulence structure of drag-reducing polymer solutions was discussed by means of the measurements of the skewness factor and the flatness factor. The skewness factor of polymer solutions showed anomalously high negative value at $y^+ = 70 \sim 120$. The corresponding flatness factor was much larger than that of water. These observations were interpreted as an increased scale of the large eddy motion in polymer solutions and as the results of suppression of sweep process because of the existence of free surface. Direct observation of fluctuating velocity and the results of one-dimensional energy spectrum confirmed the above-mentioned interpretation.

The turbulence measurements in a drag-reducing open channel flow reported in this work provided new insight into the nature of turbulence in an open channel flow. This information is expected to give the basic idea in the application of drag reduction phenomenon.

The drag reduction phenomenon caused by dilute polymer additives is well known and has been reviewed recently by Virk (1975), Little et al. (1975), and Berman (1978). The most common example of this phenomenon arises in the turbulent tube flow, where it is observed that the frictional drag at the pipe wall can be dramatically reduced. Among the various kinds of applications of this phenomenon, the drag reduction in an open channel flow is most interesting, because, if the very small amount of polymer solution is added in a water sewer, the flow rate increases at the same depth.

This enlargement of the discharge capacity should be effective for the safety of storm water sewers. Sellin and Barnard (1970) discussed the possible applications of drag reduction phenomenon to open channel flows. They found out that polymer additives caused the increase in discharge capacity not only in the tap water system but also in the sewage system. Recently, Sellin and Ollis (1979) showed that drag reduction existed even in a larger sewer (0.3 m I.D.).

Usui and Irvine (1980) carried out the experiments of drag reduction in a 90 degree isosceles triangular open channel. They measured the velocity profile of polymer solutions by means of a laser Doppler anemometer, and suggested that a considerable damping of turbulence near the free surface could exist in the case of an open channel flow. However, it was impossible to determine the value of eddy diffusivity because of the complexity in the flow geometry of their experiments.

Most previous investigations in the tube flow drag reduction (Reishman and Tiederman, 1975; Mizushina and Usui, 1977) ob-

served a significant change of wall turbulence structure, but they showed that the turbulence characteristics were almost the same as those of Newtonian fluid flows at the center portion of a tube flow. Thus, the most significant effect of drag reduction phenomenon was attributed to the increase in wall turbulence scale observed by Fortuna and Hanratty (1972), Achia and Thompson (1977), Mizushina and Usui (1977), and Berman (1980).

On the other hand, many investigations apart from the wall turbulence have been continued in the field of turbulent drag reduction. For example, Barnard and Sellin (1969) and McComb et al. (1977) discussed the effect of polymer additives in the grid generated turbulence. Usui and Sano (1980) measured the turbulent characteristics of polymer solutions in a submerged free jet, Hoyt and Taylor (1979) in a free jet discharging in air, and Chiou and Gordon (1980) in a vortex flow. All the results cited above confirmed that only a small amount of polymer additive resulted in a significant change of turbulence structure even in the free turbulent flow. From the experimental results obtained in both wall turbulence and free turbulence, it seems that the polymer additives interact with turbulent eddy in the whole range of turbulent flow field, although the interaction at the wall region is great.

An open channel flow has the characteristics both of wall bounded flow and of free surface flow. This flow system is interesting in the context of above-mentioned interaction between the polymer additives and turbulent eddy. The purpose of this work was to examine turbulent open channel flow by means of the measurements of the longitudinal fluctuating velocity. To simplify the problem in open channel flows, a rectangular open channel with large aspect ratio was used to provide essentially a two dimensional flow. It was expected that such an investigation would make clear the turbulence structure of drag reducing fluids especially near the free surface.

EXPERIMENTAL APPARATUS AND PROCEDURE

The experimental setup was just the same as reported in the previous work (Usui and Irvine, 1980) except for the test section. A once-through system including a large storage tank (1.5 m^3) was employed to minimize the mechanical degradation of polymer additives. A detailed sketch of the test section is shown in Figure 1. A rectangular open channel (4 m in length and 0.2 m in width) was used in this work. Since the maximum fluid depth was approximately 10 mm in this experiment, the aspect ratio of flow cross section was larger than 20. The slope of the flume was fixed to $s = 0.003$. All the data obtained at this slope corresponded to subcritical flow, i.e., $Fr < 1.0$. Two-dial calipers, with graduation of 0.01 mm were located at 2.2 m and 3.1 m from the channel entrance to measure the fluid depth. The fully developed condition was confirmed by checking that the fluid depth at two measuring positions coincided within 0.1 mm. The flow rate was measured by a bucket and a stop watch.

A laser Doppler anemometer similar to that previously reported (Mizushina and Usui, 1977) was used to measure the velocity distribution along the center line of the flume. The measuring station was located 2.2 m from the channel entrance. A He-Ne 5mW laser (NEO-5M) was used. The focusing and receiving optics were lenses of 250 mm focal length. A differential mode of Doppler system, with the cross angle, θ, of 6.77 degree, was used in this work. The laser beam diameter, σ, at the measuring point is, for convenience, estimated by the following equation given elsewhere (e.g., George and Lumley, 1973),

$$\sigma = \frac{2^{1/2} f_0 \lambda}{\pi d_0} \tag{1}$$

In this experiment, the focal length of the lens, f_0, wave length, λ, and the diameter of laser beam at the lens, d_0, were 250 mm, 0.6328 μm, and 1 mm, respectively. The scattering volume is usually approximated by an ellipsoid of which major axis length is σ_1, and the lengths of shorter axes are σ_2 and σ_3. Using the above-mentioned values, σ_1, σ_2 and σ_3 were estimated as 1.22, 0.072 and 0.072 mm, respectively. The major axis of scattering volume was oriented in the spanwise direction of the flume, Figure 1. The instantaneous longitudinal velocity was recorded by a data recorder (TEAC, R-61). The voltage outputs of the instrument were digitized and stored on magnetic tape. The sampling interval and the data size were 0.005 second and about 8,000, respectively. Statistical processing of the digitized data was made with TEAC, PS-80 computer syteem.

Polyethylene oxide (grade Alcox, E-160), supplied by Meisei Chemical Corp., was used as the polymer additive. The intrinsic viscosity of Alcox, E-160 in water was 1,200 cm^3/g. A stablizer, Sandex-C (Meisei Chemical Corp.), was added to prevent the chemical degradation of the polymer additive. Tap water was used to dissolve the polymer to concentrations of 50 and 100 ppm. It was certified preliminarily that Sandex-C had no effect on drag reduction in a turbulent pipe flow.

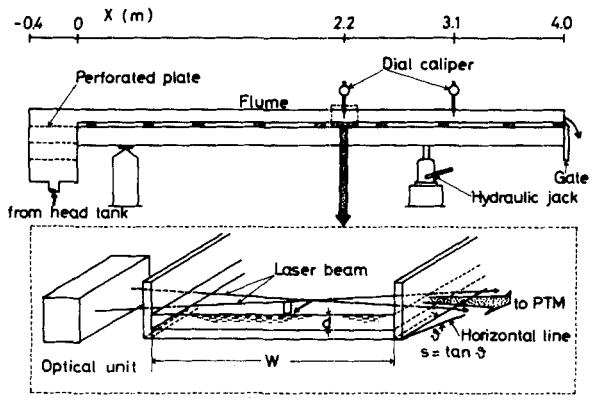

Figure 1. Experimental flume.

RESULTS AND DISCUSSION

Drag Reduction

The effect of the polymer additive on the increase in discharge capacity is shown in Figure 2. This diagram shows that only a small amount of the polymer additive causes a larger flow rate at the fixed fluid depth. The friction factor in the open channel flow was defined as

$$f = \frac{\tau_w}{\frac{1}{2}\rho U_{av}^2} = \frac{gsd_h}{2U_{av}^2} \tag{2}$$

The results shown in Figure 2 are replotted as Reynolds number vs. friction factor relationship in Figure 3. The results of water are

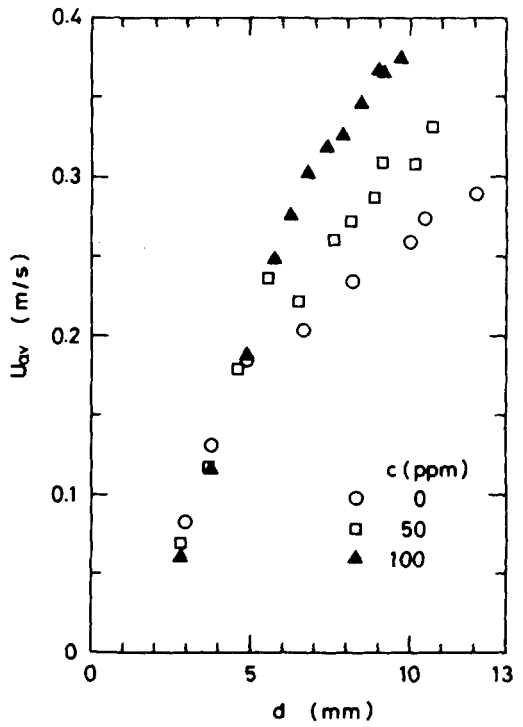

Figure 2. Effect of the polymer additive on discharge capacity in an open channel flow ($s = 0.003$).

TABLE I. EXPERIMENTAL CONDITIONS FOR THE VELOCITY MEASUREMENT RUNS

c [ppm]	d [mm]	T [K]	ν [m²/s]	U_{av} [m/s]	Re	f	$\frac{f_N^* - f_p^{**}}{f_N}$
0	10.01	294.7	9.73×10^{-7}	0.258	9660	0.00817	—
50	10.89	297.7	9.71×10^{-7}	0.308	12500	0.00528	29.5
100	9.13	296.8	10.84×10^{-7}	0.377	11600	0.00347	54.5

* f_N is the Newtonian friction factor estimated by $f = 0.0791\ Re^{-0.25}$.
** f_p is the friction factor for polymer solution.

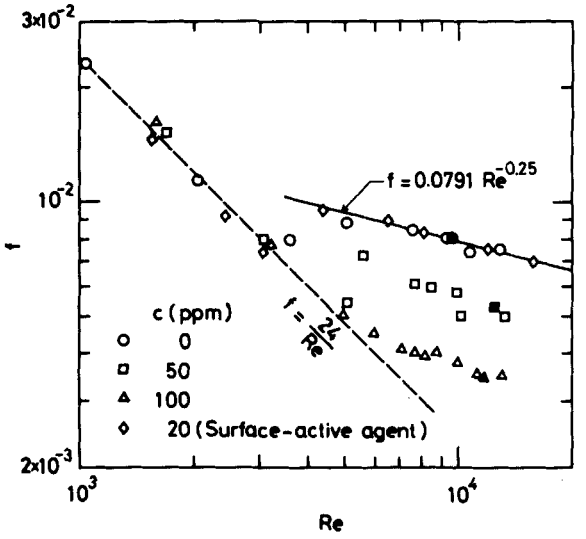

Figure 3. Drag reduction in a rectangular open channel, $s = 0.003$ (solid symbols are velocity measurement runs).

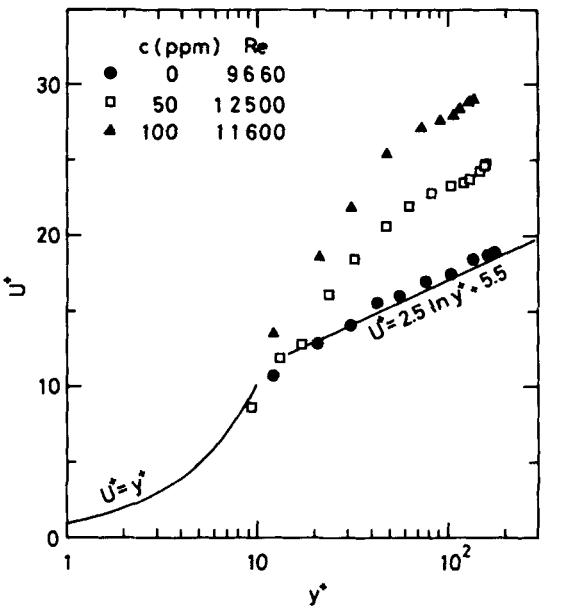

Figure 4. Velocity distribution along the center line of the flume.

in excellent agreement with the laminar friction factor between two-parallel flat plates ($f = 24/Re$), and with well-accepted turbulent friction factor ($f = 0.0791\ Re^{-0.25}$). The 100 ppm polymer solution shows almost the same behavior as the maximum drag reduction asymptote of Virk (1975). The solid symbols in this diagram indicate the run for the velocity measurements of which results will be shown in the following sections. The experimental conditions for the velocity measurements are shown in Table 1.

As it will be discussed later, the effect of the free surface on turbulent eddy seems to be large. One possibility is the change in the surface tension force caused by adding the polymer. The ratio of the surface tension force in polymer solutions to that of water was determined as 0.85 at 25°C by Du Nöuy surface tension meter. Thus, an anionic surface-active agent (grade Emal-10), supplied by Kao-Atlas Corp., was dissolved in tap water to show almost the same surface tension as that of polymer solutions. This solution with surface-active agent was also used to measure the friction factor. The results, as shown in Figure 3, coincided precisely with the data of water. Therefore, it is concluded that the change in surface tension has no effect on the amount of drag reduction.

Velocity Distribution

The results of longitudinal velocity distribution along the center line of the flume are shown in Figure 4. The velocity distributions of polymer solutions in the wall region are in essential agreement with the previous data (Virk, 1975; Berman, 1978), showing the increase in laminar sublayer or buffer layer thickness. A more distinctive feature in the velocity distribution of this work is the slight increase of velocity near the free surface. The same tendency was previously reported by Usui and Irvine (1980). This fact suggests that the turbulence structure of polymer solutions is possibly changed even near the free surface.

Turbulent Intensity

The results of turbulent intensity profiles are shown in Figure 5. One of the most reliable measurements of turbulent intensity at lower Reynolds number have given by Pennel et al. (1972), and their data is compared in this diagram. The turbulent intensity of a Newtonian fluid of this work is nearly half the previously well established value through out the whole depth of the flume.

Referring the measurements of the rate of dissipation at the center of a pipe flow by Laufer (1953), i.e., $\epsilon d_h / 2\, u^{*3} \simeq 2.5$, the

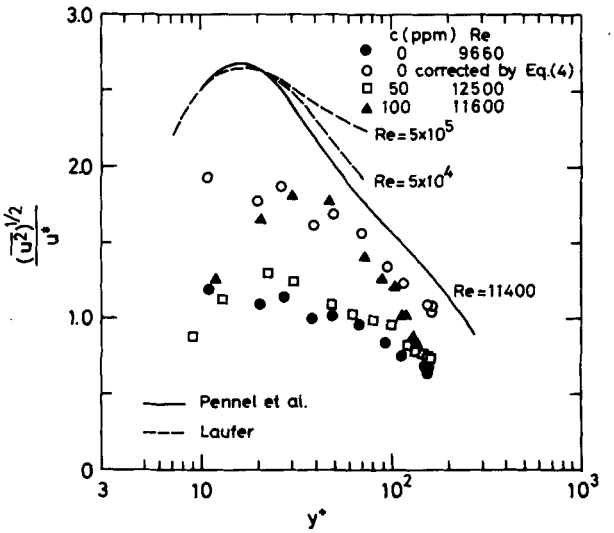

Figure 5. Turbulent intensity profile.

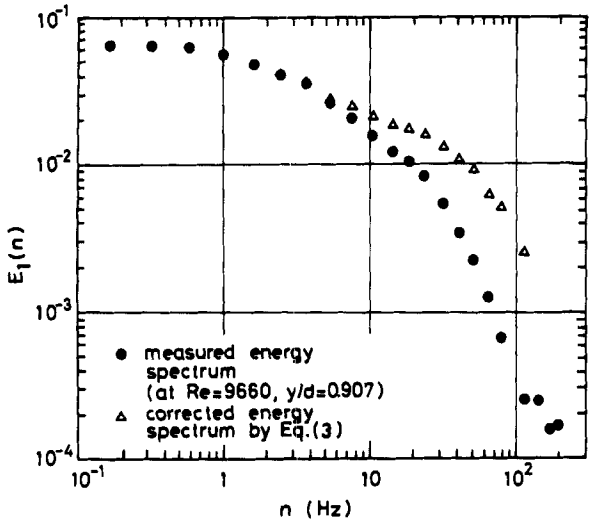

Figure 6. Effect of the finite scattering volume on one-dimensional energy spectrum in a Newtonian fluid.

Kormogoroff microscale is estimated as 0.248 mm in the case of a Newtonian fluid flow of this work (at Re = 9,660, u^* = 1.88 cm/s, d_h = 4.76 cm and ϵ = 6.96 cm^2/s^3). On the other hand, the length of major axis of the scattering volume has been estimated as 1.22 mm in the preceeding section. Thus, the spacial resolution of a laser Doppler system of this work is not enough to detect the fluctuating velocity of very small eddies. George and Lumley (1973) discussed the accuracy of flow measurements by laser Doppler measurements. Assuming the incompressible and isotropic turbulence, they gave the true one-dimensional energy spectrum, $F_{11}^1(k_1)$, and the measured one-dimensional energy spectrum, $F_0(k_1)$, by Eqs. (3.1.19) and (3.1.23) in the paper of George and Lumley (1973), respectively. Using the dimensions of the scattering volume and Kormogoroff scale of this work, the measured one-dimensional energy spectrum of this work (at Re = 9,660, y/d = 0.904) was corrected by

$$E_1(n)_{\text{corr.}} = E_1(n)_{\text{meas.}} F_{11}^1(k_1)/F_0(k_1), \tag{3}$$

and both the measured and corrected spectrum are shown in Figure 6. The results above 100 Hz are not reliable because of the Doppler ambiguous noise. Thus the integration of the energy spectrum was done from zero to 100 Hz to obtain the turbulent intensity. The ratio of the corrected intensity to the measured one was determined as

$$\frac{(\overline{u^2})^{1/2}_{\text{corr.}}}{(\overline{u^2})^{1/2}_{\text{meas.}}} = \frac{\int_0^{100} E_1(n)_{\text{corr.}}\, dn}{\int_0^{100} E_1(n)_{\text{meas.}}\, dn} = 1.60 \tag{4}$$

If this correction factor is applied throughout the whole fluid depth, the corrected turbulent intensity profile may be shown by the symbol, o, in Figure 6. Although the corrected values seem to be in agreement with the data of Pennel et al., the above-mentioned correction may not be applicable near the wall. Because the nonisotropic turbulence structure and the velocity gradient within the scattering volume should cause another significant effect on the measurements of the fluctuating velocity. The highly nonisotropic feature of the wall turbulence prevents us from the more precise discussion of the accuracy in turbulence measurements by a laser Doppler system. In conclusion, the finite dimension of the scattering volume caused a significant decrease in turbulent intensity of a Newtonian fluid in this work. Although it was desirable to use a larger flume to avoid the above-mentioned effect, the use of polymer solutions, especially in an once-through system, prevented us from using a larger flume.

In the case of polymer solutions, it is well accepted that the flow stabilizing effect of the polymer additive causes the enlargement of the turbulence scale at lower frequency and causes the suppression of the microscale eddies. This means that the same finite scattering volume can measure more correctly the turbulent intensity in the polymer solutions. The results of polymer solutions in Figure 5 indicate this tendency. However, the quantitative discussion is difficult because no information about the rate of dissipation is available in the polymer solutions. The qualitative feature of the turbulent intensity profiles in the polymer solutions corresponds well to the previous observation in drag reducing pipe flow (Reishman and Tiederman, 1975; Mizushina and Usui, 1977), showing the shift of the peak location of the turbulent intensity to the position at $y^+ = 30 \sim 50$.

Skewness Factor and Flatness Factor

It was desirable to obtain the results of statistical analysis of the digitized data for more detailed understanding of turbulence mechanism in an open channel drag reducing flow. Thus, the probability density distribution, the skewness factor and the flatness factor were calculated.

The skewness factor and the flatness factor of longitudinal fluctuating velocity are defined as:

$$S(u) = \overline{u^3}/(\overline{u^2})^{3/2} \tag{5}$$

$$F(u) = \overline{u^4}/(\overline{u^2})^2 \tag{6}$$

Since the skewness factor is an odd-order moment, it is an indication of the degree of asymmetry of the probability density distribution, and the flatness factor is the measure of the skirt of the probability density distribution. The original data of this work stored in a data recorder contained unavoidably the high frequency noise caused by the data acquisition system. The high frequency noise may be divided into two category, one is the Doppler ambiguous noise and the other is the noise caused by the signal dropout. The data acquisition system of this work is essentially the zero detector same as that described by George and Lumley (1973). Thus, the signal dropout is unavoidable, although its appearance is very scarce because of the seeding of the scattering particles. However, the spike signal caused by the signal dropout has a great effect on the value of skewness factor and flatness factor. Thus, the digitized data were filtered through a digital low pass filter process defined as

$$u(m\Delta t) = \exp(-f_c\Delta t)u((m-1)\Delta t) + \{1 - \exp(-\exp(-f_c\Delta t)\}u(m\Delta t) \tag{7}$$

where f_c is the cut frequency of a low pass filter. The value of f_c was selected as 50 Hz to obtain a good reproducibility of the skewness and flatness factors. Therefore, all the data presented hereafter do not contain the information at higher frequency fluctuations. However, as already shown in Figure 6, the measured energy spectrum was seriously affected by the finite scattering volume at higher frequency range (i.e., n > 10 Hz). Thus, the digital filter mentioned above does not make an essential change in the measured signal of velocity fluctuation. The most important problem may be the effect of the finite scattering volume on the reliability of skewness factor and flatness factor data. In the wall turbulence, it has been well accepted that the fluid motions of the bursting process, i.e., ejection and sweep, are most effective on the distribution of skewness and flatness factors. Fortuna and Hanratty (1972) have measured the transverse correlations of wall shear stress both in a Newtonian fluid and polymeric fluids in a pipe flow. They determined the integral scale of a Newtonian fluid as $\Lambda^+ = 17$ and for highly drag reducing flow as $\Lambda^+ = 62 \sim 114$. This integral scale may be interpreted as a representative scale of large eddy in the bursting process. On the other hand, the half length of the major axis of the scattering ellipsoid in this work ($\sigma_1/2$ = 0.61 mm) is nondimensionalized as $(\sigma_1 u^*/2\nu) = 11.5$ for a Newtonian fluid and 8.86 for 100 ppm polymer solution at Re = 10,000. Thus it must be concluded that the present finite scattering volume is sufficiently small to detect the large-scale motion of wall turbulence both in a Newtonian fluid and polymer solutions.

The distribution of skewness factor and flatness factor are pre-

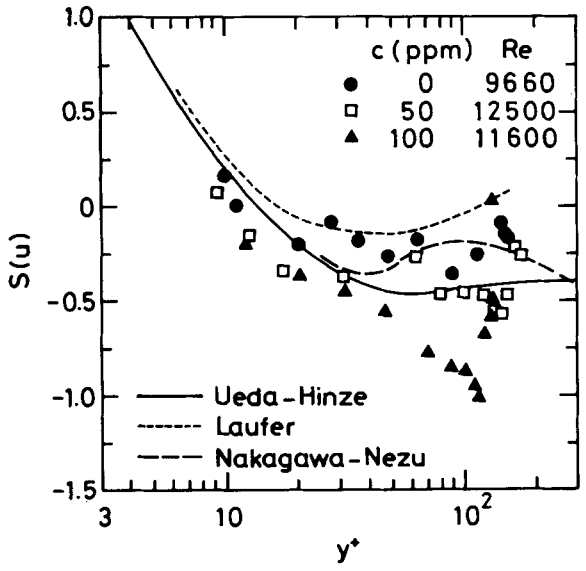

Figure 7. Distribution of the skewness factor of u.

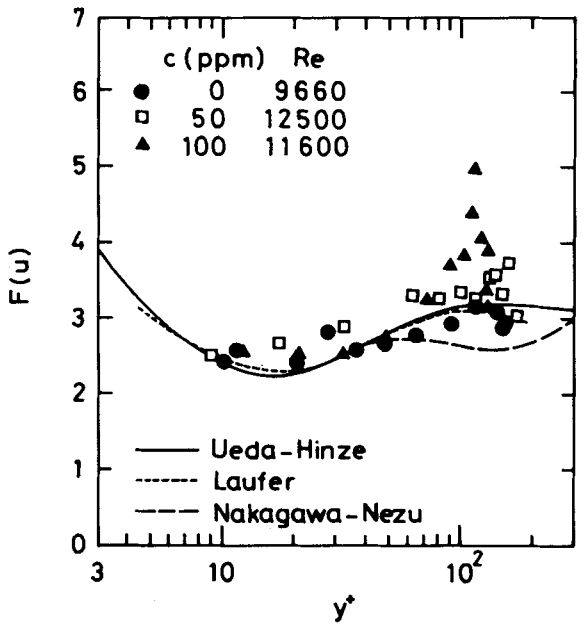

Figure 8. Distribution of the flatness factor of u.

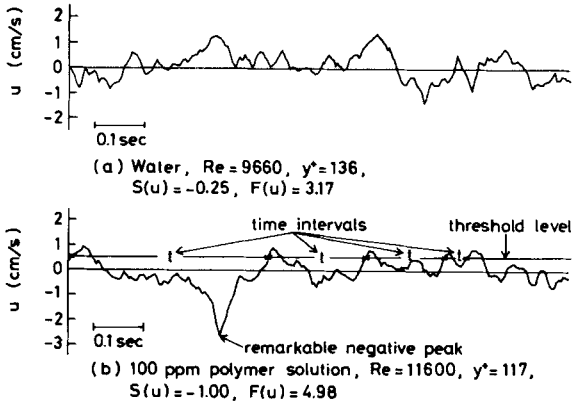

Figure 9. Fluctuation of the longitudinal velocity component.

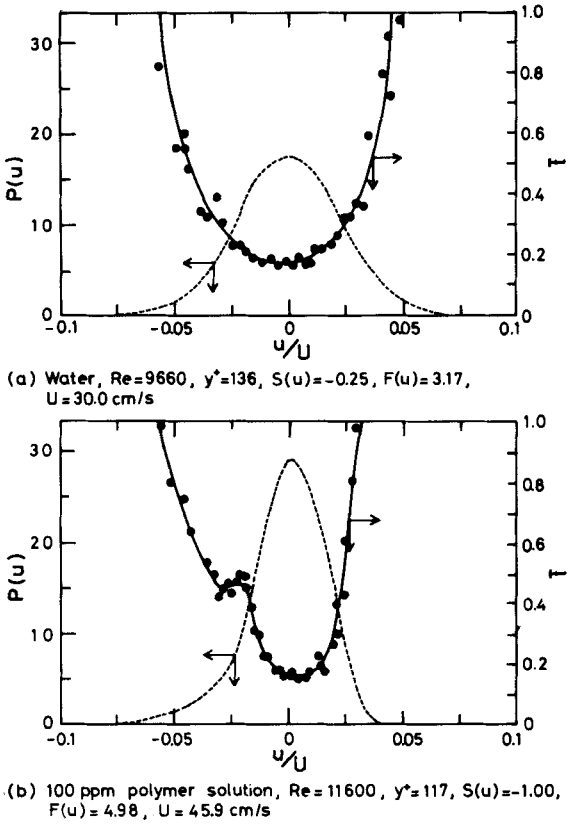

Figure 10. Probability density distribution and the mean time interval.

sented in Figures 7 and 8, respectively. The results of water are in reasonable agreement with the data of Laufer (1953), Ueda and Hinze (1975), and Nakagawa and Nezu (1977). Although the results of polymer solutions show almost the same distribution as Newtonian fluids very near the wall, the skewness factor decreases anomalously at $y^+ = 70 \sim 120$, and the flatness factor shows a remarkable increase at the same position. In addition, these distributions approach to the Newtonian values as the measuring position approaches to free surface. It is well accepted that ejection process in the large eddy motion of wall turbulence causes a negative value of the skewness factor. The above-mentioned observations mean that the effect of ejection process appears most strongly at $y^+ \simeq 100$. In the case of a 100 ppm polymer solution, the laminar sublayer and the buffer layer are thickened by the effect of polymer additive. The velocity distributions given in Figure 4 indicate that the thickness of buffer layer occupies almost the half depth of the flume. Under this condition, the ejection may lift the low velocity fluid element up to very near the free surface. However, the possibility of the inrush of the higher velocity fluid element may be very small in the turbulent core because of the existence of the free surface. Thus, in the turbulent core, the effect of ejection could appear selectively, and this seems to cause the anomalously high values of the skewness and flatness factors.

The effect of the polymer additive on the longitudinal component of the fluctuating velocity is illustrated in Figure 9. The measuring position of a 100 ppm polymer solution was located at $y^+ = 117$ or $y/d = 0.89$ where the skewness factor had the negative maximum value. In the case of water, the measuring position was selected to have almost the same value of y/d as the polymer solution. A remarkable negative peak of the fluctuating velocity is observed in the data of a 100 ppm polymer solution. It was impossible to find out the remarkable negative peak in the data of water. It was also impossible to observe such a negative peak in the data of both polymer solutions and water near the wall, although these data are not presented in this paper. The probability density distributions of the fluctuating velocity are shown in Figure 10. The experimental conditions are the same as those in Figure 9. The data of a 100 ppm polymer solution is very much skewed in the negative direction of the fluctuating velocity. Also the distributions of the mean time interval, $\bar{t}$, are shown in this diagram. The time interval

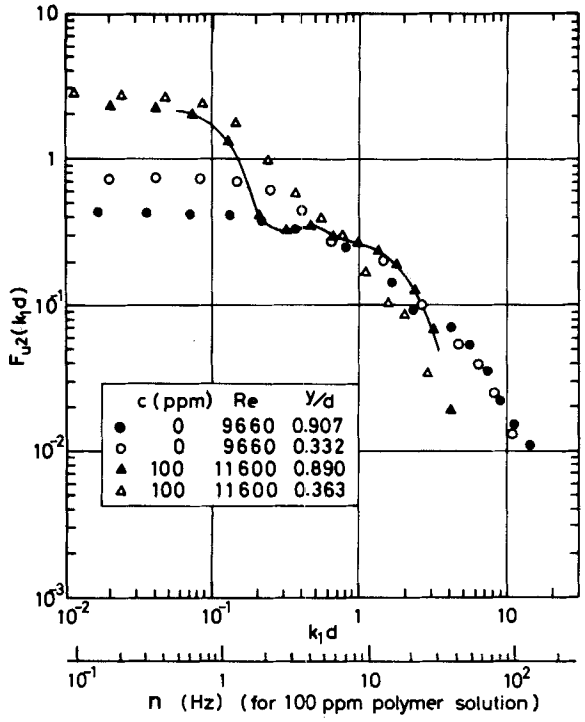

Figure 11. Distribution of one-dimensional energy spectrum.

was defined as the minimum time to cross twice the same threshold level with the same sign of (du/dt). An example of the time interval is indicated in Figure 10. The mean value of this time interval may be meaningless if the velocity fluctuation is random. However, as shown in Figure 9-b, the existence of the remarkable negative peaks in the 100 ppm polymer solution data gives almost constant time interval at $u'/U = -0.02 \sim -0.035$. This value ($\bar{t} \simeq 0.45$ s) should correspond to the mean time interval of the appearance of negative peak, and may be possibly connected with the time interval of ejection process. In the case of a Newtonian fluid (Figure 9-a), no corresponding behavior is found in the distribution of the mean time interval. In conclusion, the negative peak which appears in the turbulent core of polymer solutions seems to cause the extremely high values of the skewness and flatness factors.

To obtain the more quantitative information on the negative peak observed in Figure 9, one dimensional energy spectrum of the longitudinal fluctuating velocity was calculated. The results are shown in Figure 11. The wave number and the energy spectrum are nondimensionalized by the fluid depth, d, and the local time smoothed velocity, U, as follows:

$$F_{u^2}(k_1 d) = \frac{U}{2\pi d} \frac{E_1(n)}{\overline{u^2}} \tag{8}$$

$$k_1 d = \frac{2\pi d n}{U} \tag{9}$$

The lower horizontal axis indicated by n (Hz) is given for the case of a 100 ppm polymer solution at $y/d = 0.89$ for the convenience of the following discussion. This diagram indicates that the energy spectrum of the polymer solution at lower frequency is larger than that of water, and at higher frequency the opposite tendency is observed. These observations are well correspondent with the experimental results of McComb et al. (1977) in the grid generated turbulence. The integral scale of a 100 ppm polymer solution, which is determined from the value of energy spectrum at very low frequency, is $4 \sim 5$ times larger than that of water. More precise observation in Figure 11 gives the fact that there exists a plateau of the energy spectrum curve in the case of a 100 ppm polymer solution at $y/d = 0.89$. Such a plateau can not be found out both in the data of water at $y/d = 0.91$ or 0.33 and in the data of a polymer solution at $y/d = 0.36$. The frequency range of this plateau is given as $3 \sim 15$ Hz from the horizontal axis for n. This frequency is in good agreement with the frequency of the negative peak observed in Figure 10. The plateau in the energy spectrum curve means that the negative peaks, of which frequency is around 10 Hz, appear frequently throughout the whole data of a 100 ppm polymer solution in the turbulent core region.

Summing up the above-mentioned discussion, the effect of the ejection process is detected most strongly in the core region of turbulent drag reducing open channel flow. Although the data in the laminar sublayer was not obtained in this experiments, the skewness factor and the flatness factor of polymer solutions are expected to be almost the same as that of Newtonian fluids because the present experimental results of $S(u)$ and $F(u)$ at $y^+ = 10 \sim 20$ were not so different from that of water. The anomalous behavior of the skewness and flatness factors in the turbulent core region was interpreted as the result of suppression in sweep process caused by the effect of the free surface. More precise measurements in turbulent pipe flows or in turbulent boundary layer flows are expected for the comparison with the present experimental results in an open channel drag reducing flow.

ACKNOWLEDGMENT

The cooperation and experimental assistance of M. Kobayashi, M. Imazono and N. Iwata are gratefully acknowledged.

NOTATION

c = concentration of the polymer additive
d = fluid depth in an open channel flow
d^+ = nondimensionalized fluid depth $(= du^*/\nu)$
d_h = hydraulic diameter
d_0 = diameter of laser beam at the lens
$E_1(n)$ = one-dimensional energy spectrum
$F(u)$ = flatness factor defined by Eq. 6
Fr = Froude number $(= U_{av}/(gd)^{1/2})$
$F_{11}^1(k_1)$ = true one-dimensional energy spectrum in an isotropic turbulent flow
$F_0(k_1)$ = measured one-dimensional energy spectrum in an isotropic turbulent flow
$F_{u^2}(k_1 d)$ = nondimensionalized energy spectrum defined by Eq. 8
f = friction factor defined by Eq. 2
f_c = cut frequency of a low pass filter
f_0 = focal length of the lens
g = acceleration of gravity
k_1 = wave number $(= 2\pi n/U)$
n = frequency
$p(u)$ = probability density
Re = Reynolds number $(= d_h U_{av}/\nu)$
$S(u)$ = skewness factor defined by Eq. 5
s = slope
T = liquid temperature
$\bar{t}$ = mean time interval to cross twice the same threshold level of fluctuating velocity
Δt = data sampling interval
U = time smoothed local velocity in the longitudinal direction
U^+ = nondimensional velocity $(= U/u^*)$
U_{av} = averaged velocity over a flow cross section
u = longitudinal fluctuating velocity
u^* = wall shear velocity $(= \sqrt{\tau_w/\rho})$
W = width of a rectangular open channel
y = distance from the wall
y^+ = nondimensional distance from the wall $(= yu^*/\nu)$

Greek Letters

ϵ = rate of dissipation
η = Kormogoroff microscale $(= (\nu^3/\epsilon)^{1/4})$

θ = cross angle of two laser beams at the measuring point
Λ^+ = nondimensional integral scale of transverse space correlation in wall turbulence
λ = wave length
ν = kinematic viscosity
ρ = density
σ = laser beam diameter at the focal point
σ_1 = length of the major axis of a scattering ellipsoid
σ_2, σ_3 = length of the shorter axes of a scattering ellipsoid
τ_w = wall shear stress

LITERATURE CITED

Achia, B. U., and D. W. Thompson, "Structure of the Turbulent Boundary in Drag-Reducing Pipe Flow," *J. Fluid Mech.*, **81**, p. 439 (1977).

Barnard, B. J. S., and R. H. J. Sellin, "Grid Turbulence in Dilute Polymer Solutions," *Nature*, **222**, p. 1169 (1969).

Berman, N. S., "Drag Reduction by Polymers," *Ann. Rev. Fluid Mech.*, **10**, p. 47 (1978).

Berman, N. S., "The Effect of Sampling Probe Size on Sublayer Period in Turbulent Boundary Layers," *Chem. Eng. Commun.*, **5**, p. 337 (1980).

Chiou, C. S., and R. J. Gordon, "Vortex Flow of Dilute Polymer Solutions," *Polym. Eng. Sci.*, **20**, p. 456 (1980).

Fortuna, G., and T. J. Hanratty, "The Influence of Drag-Reducing Polymers on Turbulence in the Viscous Sublayer," *J. Fluid Mech.*, **53**, p. 575 (1972).

George, W., and J. L. Lumley, "The Laser-Doppler Velocimeter and its Application to the Measurement of Turbulence," *J. Fluid Mech.*, **60**, p. 321 (1973).

Hoyt, J. W., and J. J. Taylor, "Effect of Nozzle Shape and Polymer Additives on Water Jet Appearance," *J. Fluid Eng.*, **101**, p. 304 (1979).

Laufer, J., "The Structure of Turbulence in Fully Developed Pipe Flow," NACA TN 2954 (1953).

Little, R. C., R. J. Hansen, D. L. Hunston, O. Kim, R. L. Patterson, and R. Y. Ting, "The Drag Reduction Phenomenon. Observed Characteristics, Improved Agents, and Proposed Mechanisms," *Ind. Eng. Chem. Fund.*, **14**, p. 283 (1975).

McComb, W. D., J. Allan, and G. A. Greated, "Effect of Polymer Additives on the Small-Scale Structure of Grid-Generated Turbulence," *Phys. Fluids*, **20**, p. 873 (1977).

Mizushina, T., and H. Usui, "Reduction of Eddy Diffusion for Momentum and Heat in Viscoelastic Fluid Flow in a Circular Tube," *Phys. Fluids*, **20**, p. S100 (1977).

Nakagawa, H., and I. Nezu, "Prediction of the Contributions to the Reynolds Stress from Bursting Events in Open-Channel Flows," *J. Fluid Mech.*, **80**, p. 99 (1977).

Reishman, M. M., and W. G. Tiederman, "Laser-Doppler Anemometer Measurements in Drag-Reducing Channel Flows," *J. Fluid Mech.*, **70**, p. 369 (1975).

Sellin, R. H. J., and B. J. S. Barnard, "Open Channel Applications for Dilute Polymer Solutions," *J. Hydraulic Res.*, **8**, p. 219 (1970).

Sellin, R. H. J., and M. Ollis, "Polymer Drag Reduction in Large Pipes and Sewers," Soc. Rheol., Golden Jubilee Meeting, 37-6, Boston (1979).

Ueda, H., and J. O. Hinze, "Fine-Structure Turbulence in the Wall Region of a Turbulent Boundary Layer," *J. Fluid Mech.*, **67**, p. 125 (1975).

Usui, H., and T. F. Irvine, Jr., "Drag Reduction in a 90 Degree Triangle Open Channel," *J. Rheol.*, **24**, p. 525 (1980).

Usui, H., and Y. Sano, "Turbulence Structure of Submerged Jet of Dilute Polymer Solutions," *J. Chem. Eng. Jap.*, **13**, p. 401 (1980).

Virk, P. S., "Drag Reduction Fundamentals," *AIChE J.*, **21**, p. 625 (1975).

Diffusion of Gases in Porous Solids: Monte Carlo Simulations in the Knudsen and Ordinary Diffusion Regimes

Porous solids have been simulated in the computer as assemblages of spheres. When such assemblages contain spheres distributed in size and randomly arranged in space, the structure of the resulting solid resembles that of a real porous solid. Monte Carlo calculations of gas molecule trajectories through the assemblages were carried out for both the Knudsen and ordinary diffusion régimes. Tortuosities calculated from the simulated diffusion "data" fell in the range obtained experimentally by other investigators. Correlations were obtained that enable the prediction of diffusion rates from measurement of the porosity, mean pore size, and standard deviation of the pore size.

M. H. ABBASI and J. W. EVANS
Department of Materials Science and Mineral Engineering
University of California
Berkeley, CA

and

I. S. ABRAMSON
Department of Mathematics
University of California
San Diego, CA

SCOPE

The diffusion of gases within a porous solid is a phenomenon of practical interest in chemical engineering and metallurgical engineering, as well as in other engineering fields such as the production of energy. The presently available means for predicting rates of gaseous diffusion within porous solids are unreliable, even in the case where the structure of the porous solid is well characterized. Frequently, use is made of a "tortuosity factor," which cannot be predicted from first principles and can only be estimated with little precision, yielding diffusivities which are likely to be erroneous.

The objective of the present investigation was to remedy this situation by performing a Monte Carlo simulation of the diffusion of gas molecules in porous solids. In this procedure a